BIOLOGY OF REPRODUCTION **78,** 462–471 (2008)
Published online before print 5 December 2007.
DOI 10.1095/biolreprod.107.065771

# Comparative Analysis of Meiotic Progression in Female Mice Bearing Mutations in Genes of the DNA Mismatch Repair Pathway[1]

**Rui Kan,[4] Xianfei Sun,[4] Nadine K. Kolas,[3,4] Elena Avdievich,[5] Burkhard Kneitz,[6] Winfried Edelmann,[5] and Paula E. Cohen[2,4]**

*Department of Biomedical Sciences,[4] Cornell University College of Veterinary Medicine, Ithaca, New York 14850*
*Department of Cell Biology,[5] Albert Einstein College of Medicine, Bronx, New York 10461*
*Theodor-Boveri-Institut für Biowissenschaften,[6] Bayerische Julius-Maximilians-Universität, 97074 Würzburg, Germany*

## ABSTRACT

**The DNA mismatch repair (MMR) family functions in a variety of contexts to preserve genome integrity in most eukaryotes. In particular, members of the MMR family are involved in the process of meiotic recombination in germ cells. MMR gene mutations in mice result in meiotic disruption during prophase I, but the extent of this disruption often differs between male and female meiocytes. To address the role of MMR proteins specifically in female meiosis, we explored the progression of oocytes through prophase I and the meiotic divisions in mice harboring deletions in members of the MMR pathway (*Mlh1*, *Mlh3*, *Exo1*, and an ATPase-deficient variant of *Mlh1*, *Mlh1*$^{G67R}$). The colocalization of MLH1 and MLH3, key proteins involved in stabilization of nascent crossovers, was dependent on intact heterodimer formation and was highly correlated with the ability of oocytes to progress through to metaphase II. The exception was *Exo1*$^{-/-}$ oocytes, in which normal MLH1/MLH3 localization was observed followed by failure to proceed to metaphase II. All mutant oocytes were able to resume meiosis after dictyate arrest, but they showed a dramatic decline in chiasmata (to less than 25% of normal), accompanied by varied progression through metaphase I. Taken together, these results demonstrate that MMR function is required for the formation and stabilization of crossovers in mammalian oocytes and that, in the absence of a functional MMR system, the failure to maintain chiasmata results in a reduced ability to proceed normally through the first and second meiotic divisions, despite near-normal levels of meiotic resumption after dictyate arrest.**

*gamete biology, gametogenesis, meiosis, mismatch repair, oocyte development, ovary, recombination, synaptonemal complex*

## INTRODUCTION

Crossovers are reciprocal DNA exchange events between homologous chromosomes that occur during meiotic recombination. The appropriate distribution and frequency of crossovers, as monitored by their cytologically defined chiasmata, ensures correct chromosomal position on the meiotic spindle, proper bipolar spindle alignment, and accurate homologous segregation during meiosis I. Defects in crossover formation and placement give rise to premature random homologous segregation resulting in nondisjunction. Aneuploidy is a leading cause of infertility, spontaneous miscarriage, and congenital defects (such as Down syndrome) in humans [1, 2], and it increases susceptibility to the development of cancers in both mice and humans [3, 4]. Interestingly, 65% of aneuploidy events in Down syndrome result from errors during maternal meiosis I, and 25% of trisomy 21 cases attribute to maternal meiosis II, indicating that the human oocyte is highly susceptible to nondisjunction events [5]. However, although more than 20% of human oocytes are estimated to be aneuploid, less than 4% of human spermatozoa suffer the same fate, indicating a dramatic difference between the sexes in the success of recombination events [6, 7].

Gene targeting studies in mice have also revealed significant sex-specific differences in male and female meiosis. Genes involved in prophase I progression, such as *Spo11*, *Rad51C*, *Sycp2*, *Pms2*, and *Fkbp6*, are all essential for the survival and progression of spermatocytes through prophase I but are variably required for such events in female germ cells [8–14]. For example, FK506 binding protein 6 (FKBP6) is a component of the mammalian synaptonemal complex (SC) [10], the proteinaceous structure that appears during prophase I of meiosis and serves to tether the chromosomes together until mature crossovers are evident. Male mice harboring mutations in *Fkbp6* are sterile as a result of prophase I defects and consequent apoptosis of spermatocytes, whereas females with the mutation are fully fertile [10]. SPO11 is a conserved endonuclease that induces double strand breaks during meiosis and thereby initiates recombination. SPO11 is present in both male and female meiocytes and, presumably, functions similarly in each sex. However, whereas *Spo11*$^{-/-}$ spermatocytes undergo apoptosis during early prophase I, oocytes from *Spo11*$^{-/-}$ females show normal meiotic progression through prophase I, but most then die soon after birth [8, 9]. PMS2 is a MutL homolog of the DNA mismatch repair (MMR) pathway, and this protein also exhibits sexually dimorphic behavior during prophase I: *Pms2*-deficient females are fertile, but males are sterile because of abnormalities in the chromosome synapsis [11]. To date, no systematic study has been undertaken to compare the gender effect on chromosome segregation of different mutations affecting normal prophase I progression. However, given the prevalence of maternally derived chromosomal abnormalities arising in the human population, comparison of such events in male and female mammals is imperative for establishing potential therapies.

A number of repair pathways have been implicated in the appropriate establishment and maintenance of chiasmata, and these include proteins of the MMR pathway. The MMR protein family maintains the integrity of the genome in both prokaryotes and eukaryotes by correcting mismatched bases

[1]Supported by funding from NIH to P.E.C. (HD041012).
[2]Correspondence: FAX: 607 253 4495; e-mail: pc242@cornell.edu
[3]Current address: Centre for Systems Biology, Samuel Lunenfeld Research Institute, Mount Sinai Hospital, Toronto, ON, Canada M5G 1X5.

Received: 26 September 2007.
First decision: 22 October 2007.
Accepted: 14 November 2007.

ISSN: 0006-3363. http://www.biolreprod.org

that arise from DNA replication errors and from DNA damage (reviewed by [15]). MMR proteins also play a key role in the regulation of recombination, promotion of crossovers, and chromosome segregation in meiosis in yeasts, worms, zebrafish, and mammals [16–19]. In mammals, the MMR family is composed of the highly conserved MutS homologues (*Msh2*, *Msh3*, *Msh4*, *Msh5*, and *Msh6*) and MutL homologues (*Mlh1*, *Mlh3*, *Pms1*, and *Pms2*). In the context of meiotic recombination, only a subset of these gene products is utilized. Genetic and biochemical studies in yeasts, zebrafish, mice, and humans have indicated that the MutS homolog heterodimer of MSH4-MSH5 (MutSγ) is specifically required for homologous chromosome pairing during zygonema of prophase I in meiosis [16, 20–28]. Those MSH4-MSH5 sites stabilized by the subsequent interaction with MLH1-MLH3 heterodimers at pachynema will eventually become crossovers, whereas the other sites are thought to be processed via noncrossover pathways for double strand break resolution (reviewed by [18]).

Our previous studies show that the localization of MLH1 on SCs is dependent on the preloading of MLH3 in mouse spermatocytes, because MLH1 fails to accumulate on SCs from *Mlh3*$^{-/-}$ males [29]. By contrast, MLH3 persists on SCs from *Mlh1*$^{-/-}$ spermatocytes [29]. The downstream effectors of the MLH1-MLH3 heterodimer at sites of recombination remain unclear, however, although the 5′-3′ exonuclease, EXO1, has been implicated in these events. Studies in yeasts and mice demonstrate that EXO1 is crucial for meiotic progression through metaphase I [30–32]. *Exo1*-deficient male mice demonstrate normal meiotic progression through pachynema, but most germ cells fail to progress normally to metaphase I because of dynamic loss of chiasmata [30]. Some nonmotile spermatozoa are retrieved from epididymides of *Exo1*$^{-/-}$ males, however, suggesting that EXO1 works downstream of MSH4-MSH5 and MLH1-MLH3 in the recombination process. Female *Exo1*$^{-/-}$ mice also are sterile but display normal meiotic progression through dictyate and normal follicular development with healthy oocytes that can be recovered following hormonal stimulation by exogenous gonadotrophins [30].

To investigate the role of the MMR family in mammalian female meiosis, we have performed cytogenetic analyses of frequencies of crossovers in various mutant oocytes, compared chiasma counts between null male and female mice, and observed chromosomal configuration during metaphase using oocytes collected from *Mlh1*, *Mlh3*, *Exo1*, and *Fkbp6* mutant mice. An additional group of mice harbors a point mutation in *Mlh1* that renders the ATPase function of this protein inactive. FKBP6 was included as a point for comparison with MMR gene activity in female germ cells because *Fkbp6*$^{-/-}$ females are fertile. Importantly, this study is the first to compare all these mutant lines on a standardized C57BL/6J background, allowing for more direct comparison of the meiotic phenotypes between the mutant lines.

## MATERIALS AND METHODS

### Animals

The generation of mouse mutants and genotyping strategies for *Mlh1*, *Mlh3*, *Exo1*, and *Fkbp6* strains has been described previously [10, 12, 30, 33, 34]. All strains were housed in the Cornell University Animal Facility (Ithaca, NY), and all procedures using these mice were reviewed and approved by the Cornell University Institutional Animal Care and Use Committee. All studies were performed in accordance with the Guiding Principles for the Care and Use of Laboratory Animals. All strains of mice were maintained on the same genetic background by backcrossing heterozygote fathers with C57BL/6J mothers (Jackson Laboratories, Bar Harbor, ME) for at least six generations. Mutant mice were produced by mating heterozygous males and females. Genotyping for *Mlh1*$^{G67R/G67R}$ was performed in a 25-μl reaction that included 1× EconoTaq buffer (Lucigen, Middleton, WI), 0.2 mM deoxynucleoside triphosphates (Sigma-Aldrich, St. Louis, MO), upstream primer (P1/mlh1) at 0.8 μM, downstream primer (P2/cla1) at 0.4 μM, with 1.5 U EconoTaq DNA polymerase (Lucigen). The sequence of primers was 5′-ACT-CAGGTCCCTGGTTGGTG-3′ and 5′-AGGCCAGAGCACATTTCTGT-3′, respectively. The following PCR conditions were used: an initial incubation at 94°C for 5 min, followed by 35 cycles of denaturation at 94°C for 30 sec, annealing at 56°C for 25 sec, and extension at 72°C for 50 sec, with a final extension for 7 min. The sizes of wildtype and mutant products were 491 bp and 671 bp, respectively.

### Chromosome Analysis of Mouse Oocytes Throughout Prophase I

Chromosome preparations of oocyte nuclei were obtained by hypotonic sucrose spreading of mouse ovaries between embryonic Day 18 and Day 1 postpartum using previously published techniques [24, 29, 34]. Chromosome immunofluorescence was performed as described elsewhere [24, 29, 34]. A goat monoclonal antibody against rat SYCP3 (a component of the lateral elements of the SC), kindly provided by T. Ashley (Department of Genetics, Yale University School of Medicine, New Haven, CT), was used to identify meiotic cells. Monoclonal anti-human MLH1 (BD Pharmigen, BD Biosciences, San Jose, CA) and polyclonal rabbit anti-MLH3 [34] served to visualize late meiotic nodules. Centromeres were identified using human serum from patients with CREST (calcinosis, Raynaud phenomenon, esophageal motility disorders, sclerodactyly, telangiectasia) syndrome. All donkey-raised and fluorochrome-conjugated secondary antibodies were products of Jackson ImmunoResearch Laboratories (West Grove, PA). Immunofluorescence was visualized, captured, and scored on a Zeiss Axio Imager Z1 fluorescent microscope equipped with AxioVision 4.0 software (Carl Zeiss MicroImaging, Thornwood, NY). For all foci counts, at least 50 cells were quantified, with the exception of the *Mlh1*$^{G67R}$, which showed no MLH3 or MLH1 staining.

### Oocyte Collection, Culture, and Metaphase Analysis

Analysis of metaphase I and metaphase II oocytes was undertaken by a modification of published techniques [35, 36]. Briefly, ovaries were removed from unstimulated females at 24–26 days of age. We released oocytes by puncturing ovaries with 30-gauge needles in Waymouth media (Gibco, Invitrogen, Carlsbad, CA) supplemented with 100 U penicillin (base)/ml and 10 μg streptomycin (base)/ml, 10% fetal bovine serum (Sigma), and 0.23 mmol/L sodium pyruvate. Primary oocytes at the germinal vesicle stage were cultured in 20 μl drops of KSOM (Millipore, Bedford, MA) overlaid with mineral oil and incubated at 37°C in an atmosphere of 5% $CO_2$. After 2.5 h in culture, oocytes were transferred to fresh KSOM drops and scored for germinal vesicle breakdown (GVBD). In order to observe meiotic division at metaphase I and metaphase II, we cultured oocytes in KSOM for 8–10 h and >18 h, respectively, and fixed them in fibrin clots (see following paragraph). For metaphase II analysis, only oocytes with a single polar body were selected. Polar body extrusion rates were calculated for no fewer than 12 oocytes per genotype.

To make fibrin clots, we transferred up to 10 oocytes from KSOM to 1 μl fibrinogen solution containing 1.25% fibrinogen (Calbiochem, EMD Chemicals, San Diego, CA), 154 mM NaCl, 5.63 mM KCl, and 2.25 mM $CaCl_2$ under mineral oil on microscope slides precoated with high molecular weight poly-L-lysine (Fisher Scientific, Pittsburgh, PA). We added 1.2 μl thrombin (Sigma-Aldrich) to the fibrinogen drop and mixed gently. The mineral oil was washed off using 2% Triton X-100(Sigma)/PBS, and slides were placed in a fixative of 2% paraformaldehyde, 1% Triton X-100, 0.1 mmol/L PIPES, 5 mmol/L $MgCl_2$, and 2.5 mmol/L EGTA (Fisher) for 30 min at 37°C. Slides were washed in 0.1% normal goat serum (NGS; Gibco, Invitrogen) for 15 min at 37°C and further incubated in 10% NGS, 0.1% Triton X-100, and 0.02% sodium azide in PBS at 37°C. Then slides were either stained with antibodies or stored in 10% NGS at 4°C.

For observations of spindle morphology and chromosome configuration at metaphase I and metaphase II, oocytes were incubated with a 1:500 dilution in 5% NGS of primary mouse monoclonal antibody to β-tubulin (Sigma-Aldrich) for 1 h in a dark, humid chamber, washed three times of 10 min each in 10% NGS/PBS, and detected with a fluorescein isothiocyanate (FITC)-conjugated goat anti-mouse IgG (Jackson ImmunoResearch Laboratories, West Grove, PA). Oocytes were counterstained with 400 ng/ml 4′,6-diamidino-2-phenylindole for 2 min and dipped briefly in 0.4% Kodak Photo-flo (Electron Microscopy Sciences, Hatfield, PA). The rubber cement was removed and a coverslip applied with Prolong antifade reagent (Molecular Probes, Invitrogen). Immunofluorescence-stained slides were scored on a Zeiss Axio Imager Z1 fluorescent microscope.

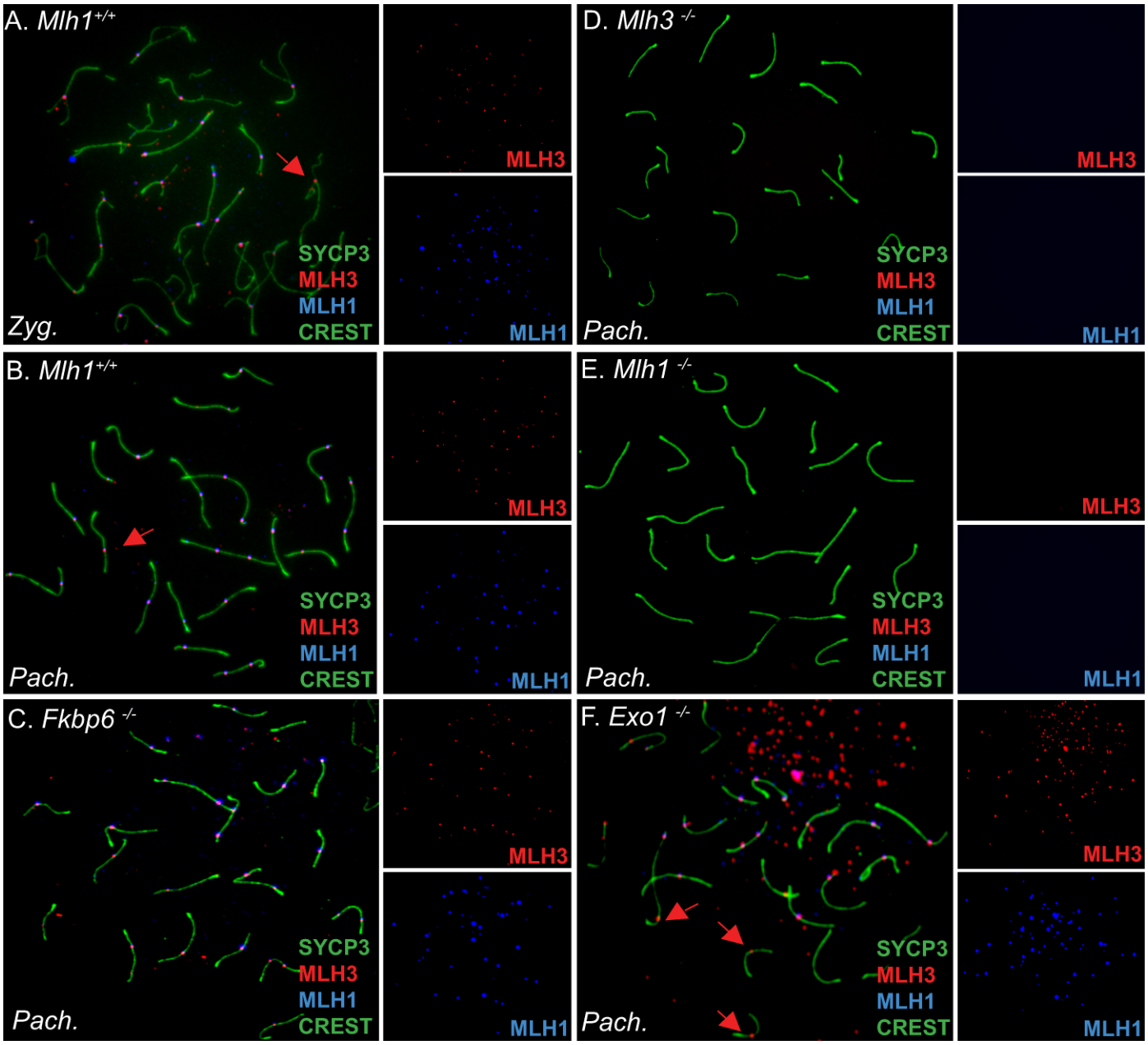


FIG. 1. Colocalization of MLH1 and MLH3 in wildtype, *Exo1*, *Fkbp6*, *Mlh1*, and *Mlh3* null mouse oocytes during prophase I. Chromosome spreads from mouse ovaries between embryonic Day 18 and Day 1 postpartum were subjected to immunofluorescent localization of SYCP3, a component of the SC (green FITC), together with MLH3 (red, Cy3), MLH1 (blue, Cy5), and CREST (green FITC). **A**) Wildtype zygonema (Zyg.) showing colocalization of MLH1 and MLH3 (overlapping signal is seen as pink) on partially synapsed SC and MLH3 focus without the companion of MLH1 (red arrow). **B**) Wildtype pachynema (Pach.) showing fully synapsed SC, appropriate numbers of MLH1/MLH3 heterodimer, and the occasional MLH3 focus in the absence of MLH1 (red arrow). **C**) Oocyte chromosome preparation at pachynema in an *Fkbp6*$^{-/-}$ female showing slightly reduced frequency of MLH1/MLH3 heterodimer. **D**) and **E**) *Mlh3*$^{-/-}$ and *Mlh1*$^{-/-}$ chromosome preparations at pachynema illustrating no localization of either MLH1 or MLH3 on SCs. **F**) *Exo1*$^{-/-}$ oocyte at pachynema showing reduced number of MLH1/MLH3 heterodimer and MLH3 foci in the absence of MLH1 (red arrows).

## *Giemsa Staining of Diakinesis-Stage Mouse Oocytes*

To analyze crossovers at diakinesis, we did chromosome preparations of oocytes, as described previously, with a slight modification [37]. Briefly, oocytes were collected and cultured for metaphase I as described earlier. After 8–10 h in culture, oocytes were transferred in a drop of 1% sodium citrate (Sigma-Aldrich) and incubated for 15 min at room temperature. Oocytes were picked up and placed in the middle of a grease-free slide. Three drops of freshly prepared fixative (three parts methanol, one part glacial acetic acid) were added onto the top of the microdrop containing oocytes. Final scattering of nuclei and spreading of chromosomes was achieved during air drying. For staining, slides were placed in Giemsa solution (Sigma) for 3 min, washed and air dried, and mounted in Histomount medium (Zymed, Invitrogen). Slides were scored on a Zeiss Axio Imager Z1 fluorescent microscope using AxioVision 4.0 software. Chiasma counts were performed on between 10 and 23 cells per genotype.

## *Giemsa Staining of Mouse Metaphase I Spermatocytes*

Adult mouse testes were decapsulated and minced in a drop of 2.3% sodium citrate. Germ cells were transferred into a fresh tube and adjusted to 3.5 ml final volume using sterile water. Cells were collected by centrifugation at 2000 rpm for 10 min and resuspended in 500 μl of 2.3% sodium citrate. We added 6 ml of 37°C prewarmed 0.075 M KCl into the tube and incubated it at 37°C for 20 min. Then cells were centrifuged and resuspended in 500 μl of 2.3% sodium citrate again. We then added 2 ml fixative of ice-cold methanol/acetic acid (three parts methanol, one part glacial acetic acid). Cells were

incubated on ice for 5 min, centrifuged, and resuspended in 500 μl of 2.3% sodium citrate. After fresh fixative was added, cells were incubated on ice for 60 min, centrifuged, and resuspended in 500 μl of 2.3% sodium citrate again. The fixative/centrifuge/resuspension step was repeated three times, but without incubation on ice. Cells were resuspended in a final volume of 500 μl of fixative, and 200 μl of cells was added onto 65°C prewarmed slides. Final scattering of nuclei and spreading of chromosomes was achieved during air drying. For staining, slides were placed in Giemsa solution for 3 min. After the slides were washed with sterile water and air dried, coverslips were applied to the slides with Histomount medium, and chromosome configurations were observed as described earlier for oocytes.

### *Quantitation and Statistical Analysis*

Immunofluorescence chromosome counts and cell staging were performed by at least three independent observers, compiled using Excel (Microsoft Corporation) and then analyzed using the statistical software package, Prism 4.0 (GraphPad Software, San Diego, CA). Staging of prophase I cells was performed according to the formation of SCs. The MLH1 and MLH3 signals distributed along chromosomes were included in our focus counts. At least 50 cells were counted for each substage of prophase I. Crossovers/chiasma counting of chromosome spreads at metaphase I was performed on oocytes or spermatocytes of at least three animals. Unpaired *t*-tests were performed to examine the variation between two groups. The statistical significance was set at $P < 0.05$.

## RESULTS

### *Frequency of MLH1-MLH3 Foci Through Prophase I in Oocytes From Wildtype and Mutant Females*

The present study was aimed at understanding the function of the MMR gene family during female meiosis and, more specifically, exploring the gender-specific responses to prophase I disruption in female and male mammals. Mutations in the MLH1-MLH3 heterodimer result in destabilization of chiasmata and loss of meiotic nodules. Although the localization of these proteins on meiotic chromosomes has been well documented for male meiotic prophase I, only limited studies have been performed to assess the localization of the MLH1-MLH3 heterodimer on meiotic chromosomes in females. We analyzed the temporal and spatial colocalization of MLH1 and MLH3 at late meiotic (or recombination) nodules using double immunofluorescent labeling techniques, in oocytes from wildtype mice, as well as those from *Fkbp6*, *Mlh3*, *Mlh1*, and *Exo1*-deficient females.

Both MLH1 and MLH3 foci were detected on the SCs of wildtype oocytes from early/mid zygonema (Fig. 1A). The mean number of foci (± SD) was 20.0 ± 6.1 for MLH1 and 20.6 ± 5.8 for MLH3, at the mid/late zygotene stage (Fig. 2). The majority of MLH3 colocalized with MLH1, but a residual number of MLH3 foci were devoid of MLH1 coimmunoreactivity (red arrow in Fig. 1A). In addition, and in contrast to what is seen in male spermatocytes [34], MLH1 is occasionally detected in the absence of MLH3 at zygonema and pachynema, but such single foci are extremely rare. The localization of MLH1/MLH3 heterodimers from early/mid zygonema in females occurs earlier than in males, where MLH3 foci appear from early pachytene and MLH1 loads at midpachytene [29, 34].

Colocalization of MLH1 and MLH3 from wildtype and MMR mutant oocytes at the pachytene stage is illustrated in Figure 1, B–F, and the quantitation is provided in Figure 2. A slight, but statistically significant, increase in MLH1 and MLH3 foci was observed in oocytes from wildtype females as prophase I progressed to pachynema, with the mean number of foci rising to 25.3 ± 4.0 and 26.8 ± 4.0, respectively (Figs. 1B and 2; $P < 0.0001$ for both MLH1 and MLH3). The number of foci was slightly lower in pachytene oocytes from *Fkbp6*$^{-/-}$ females (22.6 ± 4.2 for MLH1 and 24.2 ± 4.2 for MLH3),

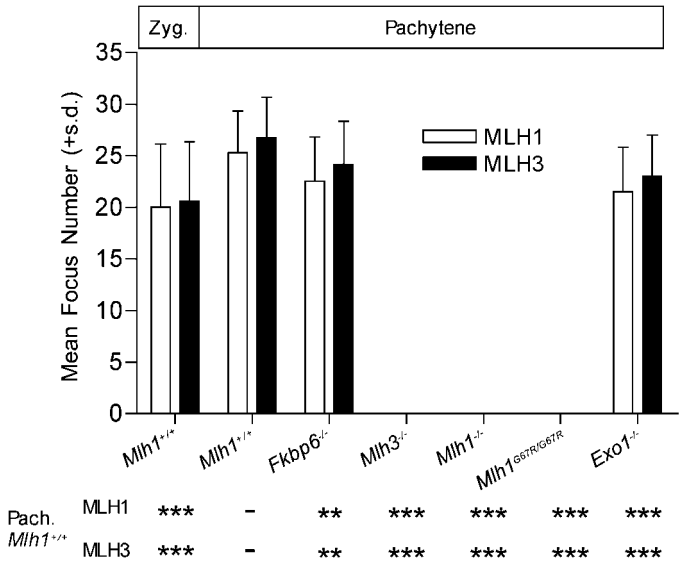


FIG. 2. Quantitation of the colocalization of MLH1 and MLH3 at prophase I from wildtype, *Exo1*, *Fkbp6*, *Mlh1*, and *Mlh3* null mouse oocytes. MLH1 and MLH3 focus numbers are significantly increased in wildtype pachynema; the loading of MLH1 onto SCs requires MLH3 in *Mlh3*$^{-/-}$ mouse oocytes. Low numbers of MLH1 and MLH3 were found in both *Fkbp6*$^{-/-}$ and *Exo1*$^{-/-}$ females, indicating that these females might have a lower frequency of chiasmata at metaphase I, and there was no statistical difference between the two. **, $P < 0.001$; ***, $P < 0.0001$. Numbers are means ± SD of at least 50 cells per genotype (except *Mlh1*$^{G67R/G67R}$ where n = 5).

and this was significant for both MLH1 and MLH3 ($P = 0.0011$ and $P = 0.0016$, respectively; Figs. 1C and 2), concurrent with the normal fertility of *Fkbp6*$^{-/-}$ females [10].

In *Mlh3*$^{-/-}$ males, MLH1 fails to load onto chromosomes of pachytene spermatocytes in the absence of MLH3, correlating with the reduction of crossovers in spermatocytes at metaphase I and subsequent sterility of these animals [34]. Similarly, in the current study, we found that both MLH1 and MLH3 were absent from pachytene chromosomes of oocytes from *Mlh3*$^{-/-}$ females (Figs. 1D and 2). In oocytes from *Mlh1*$^{-/-}$ females, we saw the appearance of very faint MLH3 foci very occasionally (Fig. 1E). Because these foci were fainter than normal MLH3 foci, and because their intensity was often below the detection threshold for our camera, these foci were not included in our quantitation (Fig. 2). However, it is important to note that, unlike the female nulls, normal intensity residual MLH3 foci are observed in *Mlh1*$^{-/-}$ males [29]. Localization of faint MLH3 foci was apparent on oocyte chromosomes of both *Mlh1* nullizygous strains (WE and ML, not shown). In view of the similar prophase I phenotypes of these mice, most prophase I studies were performed using *Mlh1*(*WE*) mice.

To investigate the role of the ATPase function of MLH1 on MLH1-MLH3 recruitment to meiotic nodules, we explored the localization of these two MutL homologs in spermatocytes of mice bearing an inactivating point mutation in the ATPase domain of the murine *Mlh1* gene. These *Mlh1*$^{G67R/G67R}$ mice are sterile and exhibit a similar meiotic phenotype to that of *Mlh1*$^{-/-}$ mice, but male spermatocytes show residual levels of MLH1 localization at pachynema in the absence of MLH3 localization (Cohen, Avdievich, Kneitz, and Edelmann, unpublished observations). In oocytes from *Mlh1*$^{G67R/G67R}$ females, however, no MLH1 or MLH3 foci were found along meiotic chromosomes during pachynema (Fig. 2), underscoring the importance of the ATPase function of MLH1 in MLH1-MLH3 dynamics.

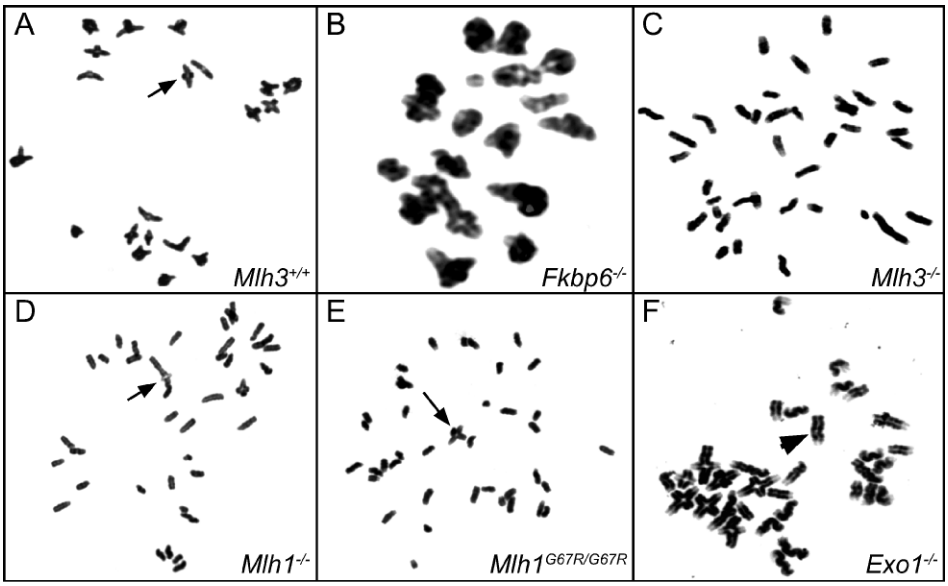


FIG. 3. Giemsa-stained preparation of diakinesis mouse oocytes, showing normal crossovers and failure to maintain crossovers in mutant mouse oocytes. **A**) Wildtype oocyte illustrating 20 bivalent diplotene chromosomes with either one chiasma (black arrow) or two chiasmata (black arrowhead) per bivalent pair. **B**) *Fkbp6*$^{-/-}$ oocyte having 20 bivalent diplotene chromosomes and normal chiasma counts. **C**) *Mlh3*$^{-/-}$oocyte showing 38 chromosomes and no crossovers, indicating the failure of recombination in the *Mlh3* null female. **D**) *Mlh1*$^{-/-}$ oocyte showing 38 chromosomes with only one bivalent diplotene chromosome with one crossover (black arrow), suggesting a failure to maintain crossovers. **E**) *Mlh1*$^{G67R/G67R}$ oocyte showing 38 chromosomes and one crossover (black arrow). **F**) *Exo1*$^{-/-}$ oocyte showing 29 chromosomes and reduced number of chiasma counts. The number of chromosomes suggests the existence of unpaired univalent chromosomes, as exemplified by the black arrowhead.

Oocytes from *Exo1*$^{-/-}$ females also showed a reduced frequency of MLH1 and MLH3 localization at pachynema of 21.5 ± 4.3 and 23.0 ± 4.0 foci, respectively (Figs. 1F and 2; $P < 0.0001$), frequencies that are not statistically different from those seen in *Fkbp6*$^{-/-}$ oocytes ($P = 0.2154$ and $P = 0.1676$, respectively). The distribution of these foci mirrors that of wildtype oocytes, with a maximum of one to two foci per chromosome, albeit it at a reduced level. Interestingly, however, the total number of MLH1 foci and MLH3 foci found in the absence of their heterodimeric partners increased in the absence of EXO1 (red arrows in Fig. 1F) from 0.6% to 2.2% and 6.0% to 8.8%, respectively (of a total of 1400 foci counted per genotype). Although these changes were not significant by $\chi^2$ analysis of total numbers of foci and were slightly significant at the $P < 0.05$ level when using Mann-Whitney *U*-tests or one-way ANOVA when comparing mean foci numbers per cell, these results suggest that EXO1 may stabilize the MLH1-MLH3 heterodimer at late meiotic nodules.

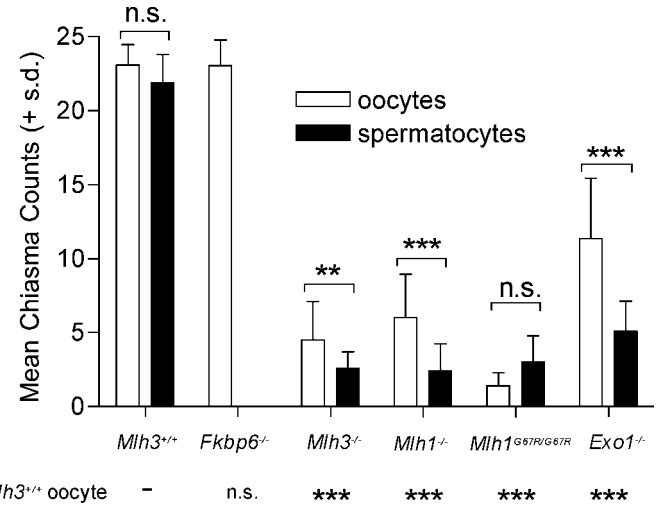


FIG. 4. Quantitation of chiasma counts at metaphase I in mutant oocytes and spermatocytes with disruption of *Exo1*, *Fkbp6*, *Mlh1*, and *Mlh3*. Defects in the MMR genes caused a significant reduction of chiasmata both in males and females, except for the *Fkbp6*$^{-/-}$ female, which has a normal number of chiasmata. The differences of chiasma frequencies between wildtype males and females and between *Mlh1*$^{G67R/G67R}$ males and females were not statistically significant. Differences in chiasma counts between males and females of the remaining genotypes were statistically significant. Frequencies of chiasmata from other mutant oocytes were dramatically decreased, in addition to those in *Fkbp6*$^{-/-}$ oocytes. ***, $P < 0.0001$; n.s., not significant. Numbers are means ± SD of at least 10 cells per genotype.

### *Chiasma Counts of Diakinesis Mouse Oocytes*

At diplonema of prophase I, the SC breaks down, and homologous chromosome interactions are maintained by the structural manifestations of homologous recombination events, the chiasmata. Lack of chiasmata and/or abnormal distribution along chromosomes causes premature homologous chromosome segregation, which, in turn, will affect spindle organization. Giemsa staining of air-dried chromosomes from diakinesis-stage oocytes from wildtype females revealed the normal crossover configurations (Fig. 3A), enabling quantitation of crossover frequency and distribution. In oocytes from wildtype mice, the 20 bivalent diplotene chromosomes usually displayed one (black arrows in Fig. 3A) or two chiasmata (arrowhead in Fig. 3A), with a mean (± SD) of 23.1 ± 1.4 (Fig. 4). Similarly, oocytes from *Fkbp6*$^{-/-}$ females had 20 bivalent diplotene chromosomes and chiasma counts that were not statistically different from those of wildtype mice (23.0 ± 1.7; $P = 0.8619$; Figs. 3B and 4). Oocytes from *Mlh1*$^{-/-}$, *Mlh1*$^{G67R/G67R}$, and *Mlh3*$^{-/-}$ females showed a failure to construct or maintain crossovers (6.0 ± 3.0, 1.4 ± 0.9, and 4.5 ± 2.6 crossovers per oocyte, respectively; Figs. 3, C–E and 4). The frequencies of chiasmata from MLH3, MLH1, and EXO1-deficient oocytes were significantly reduced ($P < 0.0001$) compared to those of wildtype and *Fkbp6*$^{-/-}$ oocytes. There was no significant difference in chiasma counts between *Mlh3* or *Mlh1* mutant females. There were more chiasmata from oocytes of *Exo1* mutant females than from oocytes of *Mlh3*, *Mlh1*, and *Mlh1*$^{G67R/G67R}$ mutant females ($P < 0.0001$), whereas there were significantly more chiasmata from oocytes of *Mlh1*$^{-/-}$ and *Mlh3*$^{-/-}$ females than from oocytes of *Mlh1*$^{G67R/G67R}$ females ($P < 0.0001$).

*Exo1*$^{-/-}$ oocytes consistently showed more than 20 chromosomes, suggesting the existence of univalent chromosomes (as shown by the arrowhead in Fig. 3F) and a concomitant reduction in the number of chiasmata (11.4 ± 4.1; Fig. 4). The frequency of chiasmata in *Exo1* null oocytes was significantly higher than in *Mlh3* and *Mlh1* null oocytes,

(A)

| Strain | Wildtype+/+ | | | Heterzygous+/- | | | Mutant-/- | | |
|---|---|---|---|---|---|---|---|---|---|
| | #oocytes collected | GVBD after 2.5hrs | Ratio(%) | #oocytes collected | GVBD after 2.5hrs | Ratio(%) | #oocytes collected | GVBD after 2.5hrs | Ratio(%) |
| *Fkbp6* | n.d. | n.d. | n.d. | 158 | 108 | 68.35 | 111 | 80 | 72.07 |
| *Mlh3* | 76 | 56 | 73.68 | 242 | 158 | 65.29 | 270 | 191 | 70.74 |
| *Mlh1*$^{G67R/G67R}$ | 57 | 48 | 84.21 | 46 | 40 | 86.96 | 206 | 177 | 85.92 |
| *Mlh1(ML)* | 50 | 30 | 60.00 | 41 | 27 | 65.85 | 48 | 24 | 50.00 |
| *Mlh1(WE)* | 100 | 69 | 69.00 | 30 | 18 | 60.00 | 27 | 8 | 29.63 |
| *Exo1* | 81 | 62 | 76.54 | 59 | 47 | 79.66 | 141 | 104 | 73.76 |
| SUM | 364 | 265 | 72.80 | 576 | 398 | 69.10 | 803 | 584 | 72.73 |

(B)

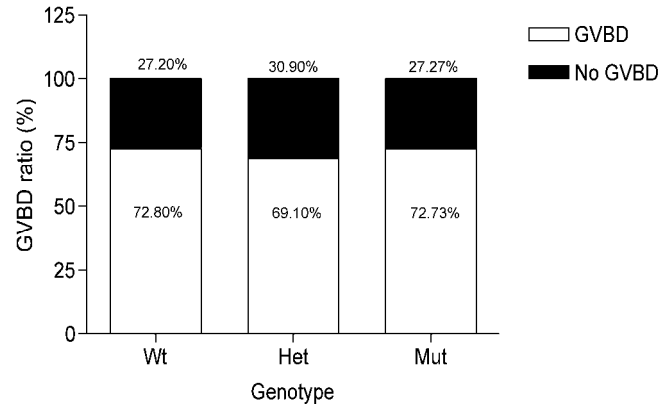


FIG. 5. Germinal vesicle breakdown in culture. Oocytes were harvested from mouse ovaries of different genotypes, and the number of those exhibiting germinal vesicle breakdown (GVBD) was scored after 2.5 h in culture. **A**) GVBD rates (%) for different genotypes of mice. **B**) Graphic representation of GVBD rates from all mutant (Mut) animals compared to all wildtype (Wt) and all heterozygous (Het) groups. n.d., not determined.

supporting the idea that EXO1 might maintain crossovers by stabilizing the MLH1-MLH3 heterodimer at late meiotic nodules.

To investigate gender effects of MMR gene deletion on female and male meiosis, we compared frequencies of chiasmata between diakinesis-stage oocytes and corresponding spermatocytes (Fig. 4). The frequency of chiasmata in wildtype females was not significantly different from that of wildtype males (23.1 ± 1.4 vs. 21.9 ± 1.9, $P = 0.093$) but might reflect an underestimate for female oocytes because of the inherent difficulties in counting these structures. Oocytes from *Fkbp6*$^{-/-}$ females had a normal number of chiasmata (23.0 ± 1.7), whereas no chiasmata could be seen in male meiocytes, given the arrest in spermatogenesis and subsequent apoptosis prior to

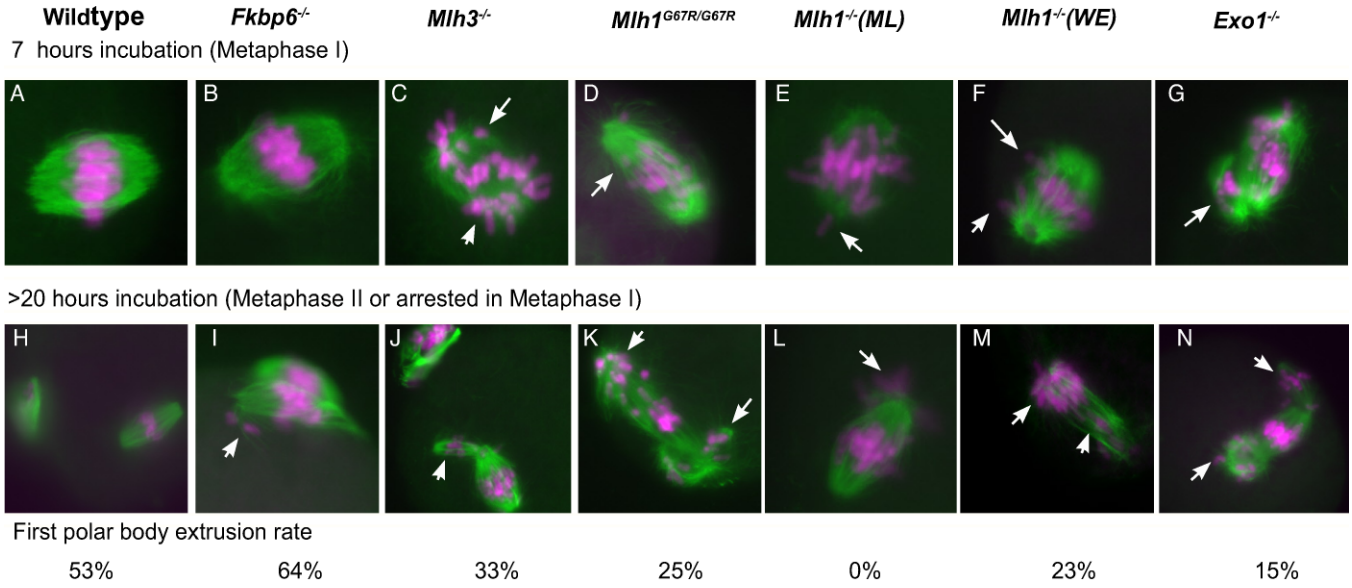


FIG. 6. Meiotic progression following GVBD in oocytes from different mutant mouse lines. Oocytes were incubated for 2.5 h in KSOM, and only those that had undergone GVBD were selected for further incubation. Panels A–G show oocytes of different genotypes in metaphase I after 7–12 h incubation: Wildtype, *Fkbp6*$^{-/-}$, *Mlh3*$^{-/-}$, *Mlh1*$^{G67R/G67R}$, *Mlh1*$^{-/-}$ (*ML*), *Mlh1*$^{-/-}$ (*WE*), and *Exo1*$^{-/-}$, respectively. Panels H–N show oocytes from the same mutant lines at later stages of meiosis after 18–22 h incubation. First polar body extrusion rates (%) are listed below for each genotype, showing the proportion of oocytes that have resumed meiosis and entered meiosis II within 22 h. The number of oocytes counted was 126 wildtype, 11 *Fkbp6*$^{-/-}$, 29 *Mlh3*$^{-/-}$, 92 *Mlh1*$^{G67R/G67R}$, 7 *Mlh1*$^{-/-}$(*ML*), 21 *Mlh1*$^{-/-}$(*WE*), and 39 *Exo1*$^{-/-}$ from between two and five females for each genotype. Arrows indicate misaligned chromosomes and/or chromosomes that are no longer chiasmate with their homolog partners.

(A)

| Genotype | # of oocytes collected | Polar body extruded | Ratio(%) |
|---|---|---|---|
| Wildtype | 126 | 67 | 53.17 |
| *Exo1*$^{-/-}$ | 39 | 6 | 15.38 |
| *Mlh1*$^{G67R/G67R}$ | 92 | 23 | 25.00 |

(B)

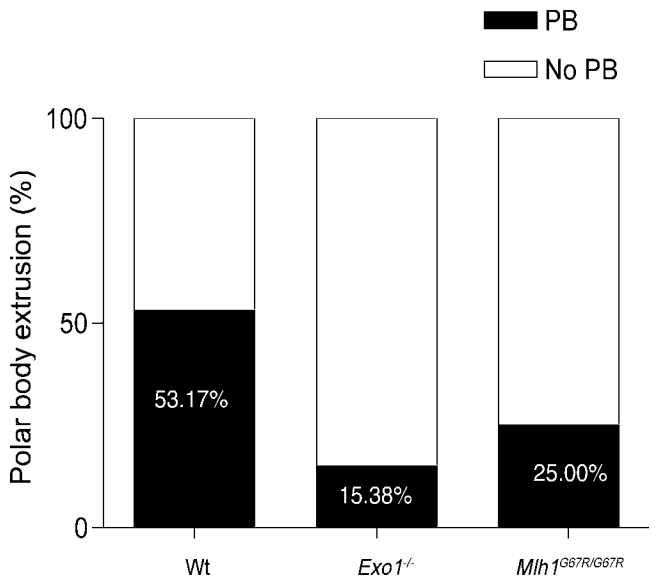


FIG. 7. Polar body (PB) extrusion rates in oocytes from wildtype, *Mlh1*$^{G67R/G67R}$, and *Exo1*$^{-/-}$ females. Oocytes were cultured for approximately 20 h post-GVBD, and the number of those that had their first polar body extruded was counted. Panel A shows the counts for each group, and panel B compares the first polar body extrusion ratio.

metaphase I. The frequency of chiasmata in *Mlh3* null females was higher than in null males (4.5 ± 2.6 vs. 2.6 ± 1.2, $P = 0.0045$), whereas chiasma counts in *Mlh1* and *Exo1*-deficient females were significantly higher than in corresponding males (6.0 ± 3.0 vs. 2.4 ± 1.8, $P < 0.0001$ and 11.4 ± 4.1 vs. 5.1 ± 2.0, $P < 0.0001$, respectively). A few crossovers exhibiting the classic cruciform configuration were found in both *Mlh3* and *Mlh1* null oocytes, suggesting the possibility of MLH1/MLH3 independent crossover pathways in mammalian meiosis.

### *Similar Rates of Germinal Vesicle Breakdown and Meiotic Resumption in Oocytes From Meiotic Mutants*

Resumption of meiosis occurred after 2.5 h incubation in oocytes from all meiotic mutant strains at a similar rate to that seen in wildtype and heterozygous oocytes. When the ability to resume meiosis was measured by GVBD, it was found that the ratio of oocytes that are able to resume meiosis was similar among different mutants and control groups (Fig. 5A). The GVBD ratio in mutant oocytes ranged from 29.63% to 73.76%, whereas the ratio was from 60% to 79.66% in the heterozygous group and from 60% to 76.54% in the wildtype group (Fig. 5A). Only oocytes from *Mlh1*(*WE*) nullizygous females showed a significant decline in GVBD ($P < 0.05$). The average of the three groups, when all mouse strains were combined, was 72.73% for oocytes from all mutant ovaries, 69.10% for the heterozygous group, and 72.80% for the wildtype group (Fig. 5B). Statistical analysis showed that no significant differences could be detected among mutant, heterozygous, and wildtype control oocytes ($\chi^2$ test, $P = 0.2824$).

### *Metaphase I and II Progression in MMR Mutant Oocytes*

Although around 72% of the mutant oocytes were able to resume meiosis, different mutants showed different aberrant metaphase configurations following meiotic resumption. At metaphase I, oocytes from *Fkbp6*$^{-/-}$ females showed no obvious chromosome or spindle aberrations and were similar morphologically to oocytes from wildtype mice (Fig. 6, A and B), which is consistent with the fertile phenotype of female mice with this gene knockout. Extrusion of the first polar body in *Fkbp6*$^{-/-}$ oocytes was also normal and occurred at a similar rate to that seen in wildtype oocytes, with 64% oocytes extruding a first polar body (Fig. 6, H and I). However, the alignment of chromosomes across the midplate in *Fkbp6*$^{-/-}$ oocytes was occasionally loose, with 25% of oocytes showing single chromosomes often misaligned along the equator at metaphase II (arrow in Fig. 6I).

In contrast to the relatively normal picture for *Fkbp6* null animals, oocytes from *Mlh3*$^{-/-}$ ovaries showed severely aberrant spindle configurations after 7 h of culture. This is exemplified in Figure 6C, which shows an oocyte with an abnormal distribution of chromosomes around the metaphase I spindle (white arrows). Approximately 66% of the oocytes from *Mlh3*$^{-/-}$ mice arrested at metaphase I, whereas the remainder proceeded through to metaphase II (data not shown). In those oocytes that progressed through to metaphase II, the dispersal of chromosomes throughout the oocyte cytoplasm often led to second spindle formation within the oocyte itself, as demonstrated in Figure 6J (white arrow).

Oocytes from *Mlh1*$^{G67R/G67R}$ females showed congression failure similar to that reported for oocytes from *Mlh1*$^{-/-}$(*ML*) females [35] (Fig. 6D, white arrow), and most (>75%) failed to enter meiosis II and, instead, arrested at the first meiotic division without polar body extrusion. Many arrested oocytes presented with abnormally elongated spindle configurations (Supplemental Figure 1 available at www.biolreprod.org). As seen in oocytes from *Mlh3*$^{-/-}$ females, the disarray of chromosomes around the metaphase I spindle often resulted in multiple spindle formation within the same oocyte at metaphase II (Fig. 6K, white arrows).

Previous studies demonstrated severe congression failure in oocytes from *Mlh1*$^{-/-}$ females [35]. The mice used by Woods et al. [35] were one of two nullizygous mutant lines generated and described previously [12, 33]. These mice are termed *Mlh1*(*ML*) mice herein to reflect the source of the mutant line (the laboratory of Michael Liskay). To compare these mice to the second mutant line, termed *Mlh1*(*WE*) (from the laboratory of Winfried Edelmann), oocytes were analyzed for meiotic progression and spindle assembly. Oocytes from *Mlh1*$^{-/-}$(*ML*) females exhibited severe defects in chromosome alignment, as previously reported [35] (Fig. 6E) but with less chromosomal disarray than seen in oocytes from *Mlh3*$^{-/-}$, *Mlh1*$^{G67R/G67R}$, and *Exo1*$^{-/-}$ (see following) females. All the oocytes failed to enter meiosis II and arrested in metaphase I, exemplified by the oocyte in Figure 6L, which shows two groupings of chromosomes, one at the equator and one at one spindle pole. By contrast, most chromosomes aligned at the equator in oocytes from *Mlh1*$^{-/-}$(*WE*) females, with only a few chromosomes deviating from the spindle (Fig. 6F), but these oocytes still arrested at metaphase, as shown by a reduced rate of first polar body extrusion (23%; Fig. 6M and Supplemental Fig. 1D). Thus, *Mlh1*(*ML*) mutant oocytes had a lower first polar body

extrusion rate than that seen in *Mlh1*(*WE*) mutant oocytes (0/7, 3/13, respectively). Furthermore, abnormal multiple spindle structures were observed at metaphase II in *Mlh1*(*WE*) mutant oocytes but not in *Mlh1*(*ML*) mutant oocytes.

Oocytes from *Exo1*$^{-/-}$ females showed loose arrangement of chromosomes in metaphase I (Fig. 6G), with chromosomes scattered around the spindle and multiple groupings of chromosomes throughout the oocyte. Approximately 85% of the mutant oocytes arrested in metaphase I and had aberrant spindles (Fig. 6N). For those oocytes that extruded first polar bodies and then arrested normally at metaphase II, single chromosomes could often be seen away from the meiotic equator (Supplemental Fig. 1A).

### *Polar Body Extrusion Rates in Oocytes From* Mlh1$^{G67R/G67R}$ *and* Exo1$^{-/-}$ *Females*

Our observations of meiotic mutant females showed that the mutant oocytes were able to start meiosis I, but more than half of the oocytes failed to reach metaphase II. In oocytes from *Exo1*$^{-/-}$ mutant females, this meiotic disruption was the most dramatic, with approximately 15% of oocytes extruding a first polar body within 20 h of incubation. By contrast, the first polar body extrusion rate was 75% for heterozygote *Mlh1*$^{+/G67R}$ females (not shown) and 53% for the wildtype group (Fig. 7). The reduction in polar body extrusion rates seen in the homozygous mutant animals is significantly lower than that seen in wildtype controls ($\chi^2$, $P < 0.0001$).

## DISCUSSION

The current study was aimed at comparing meiotic progression beyond prophase I in female mouse mutants exhibiting defects in synapsis and recombination. Previous studies have focused almost exclusively on prophase I disruption in male mutants, with little beyond preliminary observations in females. In all the mutants examined herein, it is noteworthy that the homozygous males all exhibited late prophase I or early metaphase I arrest [12, 29, 34], whereas oocytes bearing the same mutation can progress through much of metaphase I and, in the case of *Fkbp6* deletion, can produce viable offspring.

To compare meiotic prophase I progression in oocytes from each of the mutant mouse lines described herein, we first analyzed the progression of meiotic recombination by assessing the localization of MLH1 and MLH3 at meiotic nodules through prophase I. Using dual labeling immunofluorescence of each MutL homolog simultaneously, coupled with immunofluorescent labeling of the SC with anti-SYCP3 antibodies, we have visualized the appearance and frequency of foci of each MutL homolog together with the frequency of their colocalization across the chromosome cores. As observed for male spermatocytes, the number of MLH1 and MLH3 foci in late pachynema was equivalent in oocytes from wildtype females (Figs. 1 and 2), indicating their colocalization at late meiotic nodules. However, the appearance of MLH1/MLH3 dual-labeled foci at zygonema was earlier than that reported for MLH1 or MLH3 in pachytene spermatocytes [12, 29, 34], suggesting that the establishment of late meiotic nodules, and therefore the cohort of double strand break sites that will become sites of crossing over, occurs earlier in females than in males. The earlier specific timing for MLH1/MLH3 appearance in female germ cells was reported by our previous studies in human oocytes in which MLH1 and MLH3 were shown to accumulate on meiotic chromosomes in early zygonema [24]. The current studies now show that a similar temporal appearance of MLH1/MLH3 occurs in mice and that the timing of MLH1/MLH3 recruitment occurs earlier in female mouse meiocytes than in males. That such sites might mature earlier in females than in males might explain why premature failure of SC events in females, as seen in *Sycp3*$^{-/-}$ animals, does not affect chromosome segregation to the same extent that it does in males [38, 39]. This is exemplified in the current study by oocytes from *Fkbp6*$^{-/-}$ females, in which the normal appearance of MLH1 and MLH3 at zygonema and pachynema (Fig. 2), despite poor SC formation [10], results in oocytes that are viable and can produce normal offspring, whereas spermatocytes from *Fkbp6*$^{-/-}$ males are eradicated prior to the first meiotic division [10].

As expected, and as observed in male meiocytes [29, 34], oocytes from *Mlh3*$^{-/-}$ females showed no accumulation of either MLH1 or MLH3 on meiotic chromosomes at pachynema. However, oocytes from *Mlh1*$^{-/-}$ females also showed a failure to load MLH3, which is in contrast to what is seen in *Mlh1*$^{-/-}$ males, in which MLH3 loads independently of MLH1 [29, 34]. Indeed, our current observations of oocytes from wildtype females suggest some transient, if unstable, loading of MLH1 in the absence of MLH3. This would suggest that MLH1 and MLH3 load almost simultaneously onto chromosome cores of female meiocytes but sequentially (first MLH3 then MLH1) onto chromosome cores of male meiocytes. Furthermore, the observation that neither MLH1 nor MLH3 load onto chromosomes in mutants bearing an ATPase-defective form of MLH1 (*Mlh1*$^{G67R/G67R}$) indicates that the ATPase function of MLH1 is essential for MLH1/MLH3 deposition on prophase I chromosomes. Interestingly, EXO1 also may be required for MLH1/MLH3 stabilization at meiotic nodules, because this protein is thought to function after MLH1/MLH3, and yet mutant oocytes showed a significant reduction in MLH1/MLH3 foci at pachynema (Fig. 2; discussed later).

The failure of prophase I events in female meiocytes, as observed in the current cohort of mutant mouse strains, does not prevent the progression of these oocytes through to metaphase following dictyate arrest. Indeed, when oocytes were obtained by follicular puncture from postnatal unstimulated ovaries and were cultured in vitro, oocytes from most homozygous mutant animals were able to resume meiosis as efficiently as those from wildtype littermates. However, oocytes from both *Mlh1* nullizygous lines were slightly [and for *Mlh1*(*WE*) nulls, significantly] impaired in the ability to undergo GVBD compared to wildtype and mutant oocytes from other strains, but this might reflect errors in meiotic recombination or in failure to repair DNA mismatches created at replication.

Following the resumption of prophase I in postnatal ovaries, oocytes progressed through the first meiotic division rapidly in culture. The absence of MLH1 or MLH3 resulted in a high proportion of oocytes stalled at the first meiotic division, with only 23%–33% of oocytes from *Mlh1*(*WE*)$^{-/-}$ and *Mlh3*$^{-/-}$ extruding a first polar body. Interestingly, even fewer oocytes from *Mlh1*(*ML*)$^{-/-}$ were capable of progressing through the first meiotic division, in line with previous reports of this mutant mouse line [35]. In the current study, all lines of mice have been previously backcrossed onto the C57BL/6J background, precluding any strain differences between the mice. Thus, the difference between the two *Mlh1* nullizygous lines most probably reflects subtle differences in the strategy for ablating the *Mlh1* allele. It is important to note in this context that all oocytes for meiotic resumption studies were obtained by ovarian puncture from unstimulated females, followed by culture of the oocytes in vitro for up to 20 h, precluding any effects of gonadotrophin stimulation or other treatment (such as hyaluronidase removal of granulosa cells)

on the ability of oocytes to resume meiosis and undergo the first meiotic division. Given these strict experimental constraints, it can be concluded that less than 25% of oocytes can proceed through the first meiotic division in the absence of MLH1 or MLH3 or even in the absence of fully functional MLH1 (as in the $Mlh1^{G67R/G67R}$ mice), whereas less than 15% of oocytes can undergo the first meiotic division in the absence of EXO1.

Analysis of $Mlh1^{G67R/G67R}$ female mice revealed important functions for the ATPase domain of MLH1 in mammalian meiosis. Despite the formation of MLH1 protein in these mice, MLH1 and MLH3 still failed to accumulate at late meiotic nodules. This is manifested by a more severe loss of chiasmata in oocytes from these animals compared to that seen in either $Mlh1^{-/-}$ or $Mlh3^{-/-}$ females. In $Mlh1^{G67R/G67R}$ males, MLH1 also failed to accumulate normally at meiotic nodules, but occasional MLH1 foci were observed at severely reduced intensity without concurrent MLH3 colocalization (Avdievich et al., unpublished data). These weakly staining MLH1 foci were not observed in $Mlh1^{G67R/G67R}$ females, suggesting that the accumulation of MLH1 and MLH3 on meiotic chromosome cores in males and females is regulated differently, either because the selection of meiotic nodules for further processing through the MLH1/MLH3 pathway is determined via different mechanisms or because the stabilization of MLH1/MLH3 at meiotic nodules varies in male versus female germ cells. Because MLH1 and MLH3 accumulate simultaneously on meiotic chromosomes in oocytes but sequentially in spermatocytes, it is tempting to speculate that the requirements for an ATPase-competent MLH1 in oocytes allow for loading of the MutL heterodimer, whereas in males the equivalent functional component of the MLH3 protein drives MutL heterodimer loading.

The function of EXO1 during meiotic prophase I has remained elusive in both male and female mice [30]. EXO1 is a 5′-3′ exonuclease that interacts with MutS and MutL homologs and has been implicated in the excision step of DNA mismatch repair. EXO1 also appears to function in other repair pathways that are independent of the MMR machinery [40, 41]. During meiosis, EXO1 is required in the later stages of prophase I because spermatocytes from *Exo1*-deficient males exhibit meiotic disruption as a result of dynamic loss of chiasmata during metaphase I, resulting in meiotic failure and apoptosis [30]. The biological function of EXO1 at the level of crossing over is not clear, however, the current studies implicate EXO1 in events that result in the stabilization of crossovers after accumulation of MLH1 and MLH3. A stabilization function of Exo1 has also been proposed for the assembly of mitotic multiprotein complexes containing MMR proteins [42]. Such a function is also supported by the current data showing that, despite the near-normal accumulation and/or retention of MLH1 and MLH3 on chromosome cores during prophase I in oocytes from $Exo1^{-/-}$ females, the number of residual chiasmata in these oocytes at diakinesis remained significantly lower than that seen in wildtype oocytes (Fig. 4) but was significantly elevated above that seen in spermatocytes from $Exo1^{-/-}$ males and above that seen in oocytes from $Mlh1^{-/-}$ and $Mlh3^{-/-}$ females (Fig. 4). Thus, normal recombination events in $Exo1^{-/-}$ oocytes are lost as a result of destabilization of the MLH1/MLH3 heterodimer at a subset of the late meiotic nodules. The remaining nodules in $Exo1^{-/-}$ females are capable of giving rise to a reduced number of chiasmata at diakinesis (approximately half that seen in wildtype oocytes), but these are not sufficient to ensure successful segregation at the first meiotic division. The resulting oocytes in $Exo1^{-/-}$ females are incapable of giving rise to normal fertilized oocytes [30], with less than 15% of these oocytes progressing beyond the first meiotic division. Importantly, these studies are the first to show that normal accumulation of MLH1 and MLH3 on SCs at pachynema is not always predictive for proper chiasma formation and maintenance.

The increased failure rate of meiotic resumption in $Exo1^{-/-}$ females compared to either $Mlh1^{-/-}$ or $Mlh3^{-/-}$ females is surprising, given the higher incidence of chiasmata in EXO1-deficient oocytes, but it indicates that EXO1 functions downstream of the MutL homologs during meiotic prophase and suggests that EXO1 may stabilize crossover events after the breakdown of the SC and/or might facilitate dissolution of chiasmata at metaphase I. Furthermore, these observations indicate that once MLH1/MLH3-dependent crossover events have been selected from all the possible double strand break events genome-wide, they cannot then be diverted to an alternative pathway for processing, such as noncrossover pathways or MLH1/MLH3-independent crossover pathways. Cytogenetic and genetic analysis of recombination events in murine meiosis have shown that approximately 10% of all crossovers are independent of MLH1 [43] and MLH3 (Svetlanov and Cohen, unpublished data) but that these sites are selected prior to MLH1/MLH3 accumulation on meiotic chromosome cores. At the same time, noncrossover events, which also do not appear to require MLH1/MLH3 (at least in yeasts), are also selected prior to the loading of this MutL heterodimer. Thus, given that crossover events in EXO1-deficient oocytes fail after MLH1/MLH3 loading, it appears that these events cannot be diverted via one of these other recombination pathways. Instead, in males, EXO1-deficient spermatocytes are eradicated by apoptosis, whereas in $Exo1^{-/-}$ females, oocytes attempt to progress through the first meiotic division without appropriate chiasmata to ensure accurate segregation of bivalent diplotene chromosomes.

In summary, these studies illustrate important temporal differences in, and functional requirements for, the recruitment of MLH1/MLH3 to sites of recombination in mammalian meiocytes. Such differences might account for the increased stringency of checkpoint mechanisms in male germ cells relative to their female counterparts. Furthermore, these studies demonstrate that EXO1 plays a vital role downstream of MLH1/MLH3 in maintaining nascent crossover structures and may be important for the resolution of crossing over at metaphase I. Finally, these studies document the heterogeneous cytological consequences of such prophase I disruption on the resumption of meiosis and progression through the first and second meiotic divisions. Given the high frequency of errors seen in these processes in humans, the current studies lend credence to the idea that genetic alterations in prophase I regulation, through subtle variations in key recombinogenic genes, might account for many of the reported defects observed in human oocytes.

## ACKNOWLEDGMENTS

We thank Terry Ashley (Yale University, New Haven, CT) for the generous gift of antibodies and Josef Penninger (Institute of Molecular Biology of the Austrian Academy of Sciences, Vienna, Austria) and Michael Liskay (Oregon Health Sciences University, Portland, OR) for providing us with *Fkbp6* and *Mlh1* null mouse lines.

## REFERENCES

1. Lynn A, Ashley T, Hassold T. Variation in human meiotic recombination. Annu Rev Genomics Hum Genet 2004; 5:317–349.
2. Hassold T, Abruzzo M, Adkins K, Griffin D, Merrill M, Millie E, Saker D, Shen J, Zaragoza M. Human aneuploidy: incidence, origin, and etiology. Environ Mol Mutagen 1996; 28:167–175.

3. Gollin SM. Mechanisms leading to chromosomal instability. Semin Cancer Biol 2005; 15:33–42.
4. Venkitaraman AR. Chromosomal instability in cancer: causality and interdependence. Cell Cycle 2007; 6:2341–2343.
5. Hassold T, Hunt P. To err (meiotically) is human: the genesis of human aneuploidy. Nat Rev Genet 2001; 2:280–291.
6. Plachot M. Chromosomal abnormalities in oocytes. Mol Cell Endocrinol 2001; 183(suppl 1):S59–S63.
7. Martin RH, Ko E, Rademaker A. Distribution of aneuploidy in human gametes: comparison between human sperm and oocytes. Am J Med Genet 1991; 39:321–331.
8. Romanienko PJ, Camerini-Otero RD. The mouse Spo11 gene is required for meiotic chromosome synapsis. Mol Cell 2000; 6:975–987.
9. Baudat F, Manova K, Yuen JP, Jasin M, Keeney S. Chromosome synapsis defects and sexually dimorphic meiotic progression in mice lacking Spo11. Mol Cell 2000; 6:989–998.
10. Crackower MA, Kolas NK, Noguchi J, Sarao R, Kikuchi K, Kaneko H, Kobayashi E, Kawai Y, Kozieradzki I, Landers R, Mo R, Hui CC, Nieves E, Cohen PE, Osborne LR, Wada T, Kunieda T, Moens PB, Penninger JM. Essential role of Fkbp6 in male fertility and homologous chromosome pairing in meiosis. Science 2003; 300:1291–1295.
11. Baker SM, Bronner CE, Zhang L, Plug AK, Robatzek M, Warren G, Elliott EA, Yu J, Ashley T, Arnheim N, Flavell RA, Liskay RM. Male mice defective in the DNA mismatch repair gene *PMS2* exhibit abnormal chromosome synapsis in meiosis. Cell 1995; 82:309–319.
12. Baker SM, Plug AW, Prolla TA, Bronner CE, Harris AC, Yao X, Christie DM, Monell C, Arnheim N, Bradley A, Ashley T, Liskay RM. Involvement of mouse Mlh1 in DNA mismatch repair and meiotic crossing over. Nat Genet 1996; 13:336–342.
13. Yang F, De La Fuente R, Leu NA, Baumann C, McLaughlin KJ, Wang PJ. Mouse SYCP2 is required for synaptonemal complex assembly and chromosomal synapsis during male meiosis. J Cell Biol 2006; 173:497–507.
14. Kuznetsov S, Pellegrini M, Shuda K, Fernandez-Capetillo O, Liu Y, Martin BK, Burkett S, Southon E, Pati D, Tessarollo L, West SC, Donovan PJ, Nussenzweig A, Sharan SK. RAD51C deficiency in mice results in early prophase I arrest in males and sister chromatid separation at metaphase II in females. J Cell Biol 2007; 176:581–592.
15. Kunkel TA, Erie DA. DNA mismatch repair. Annu Rev Biochem 2005; 74:681–710.
16. Zalevsky J, MacQueen AJ, Duffy JB, Kemphues KJ, Villeneuve AM. Crossing over during Caenorhabditis elegans meiosis requires a conserved MutS-based pathway that is partially dispensable in budding yeast. Genetics 1999; 153:1271–1283.
17. Kearney HM, Kirkpatrick DT, Gerton JL, Petes TD. Meiotic recombination involving heterozygous large insertions in Saccharomyces cerevisiae: formation and repair of large, unpaired DNA loops. Genetics 2001; 158: 1457–1476.
18. Kolas NK, Cohen PE. Novel and diverse functions of the DNA mismatch repair family in mammalian meiosis and recombination. Cytogenet Genome Res 2004; 107:216–231.
19. Surtees JA, Argueso JL, Alani E. Mismatch repair proteins: key regulators of genetic recombination. Cytogenet Genome Res 2004; 107:146–159.
20. Kneitz B, Cohen PE, Avdievich E, Zhu L, Kane MF, Hou H Jr, Kolodner RD, Kucherlapati R, Pollard JW, Edelmann W. MutS homolog 4 localization to meiotic chromosomes is required for chromosome pairing during meiosis in male and female mice. Genes Dev 2000; 14:1085–1097.
21. Snowden T, Acharya S, Butz C, Berardini M, Fishel R. hMSH4-hMSH5 recognizes Holliday junctions and forms a meiosis-specific sliding clamp that embraces homologous chromosomes. Mol Cell 2004; 15:437–451.
22. Edelmann W, Cohen PE, Kneitz B, Winand N, Lia M, Heyer J, Kolodner R, Pollard JW, Kucherlapati R. Mammalian MutS homologue 5 is required for chromosome pairing in meiosis. Nat Genet 1999; 21:123–127.
23. de Vries SS, Baart EB, Dekker M, Siezen A, de Rooij DG, de Boer P, te Riele H. Mouse MutS-like protein Msh5 is required for proper chromosome synapsis in male and female meiosis. Genes Dev 1999; 13: 523–531.
24. Lenzi ML, Smith J, Snowden T, Kim M, Fishel R, Poulos BK, Cohen PE. Extreme heterogeneity in the molecular events leading to the establishment of chiasmata during meiosis I in human oocytes. Am J Hum Genet 2005; 76:112–127.
25. Ross-Macdonald P, Roeder GS. Mutation of a meiosis-specific MutS homolog decreases crossing over but not mismatch correction. Cell 1994; 79:1069–1080.
26. Hollingsworth NM, Ponte L, Halsey C. MSH5, a novel MutS homolog, facilitates meiotic reciprocal recombination between homologs in Saccharomyces cerevisiae but not mismatch repair. Genes Dev 1995; 9: 1728–1739.
27. Bocker T, Barusevicius A, Snowden T, Rasio D, Guerrette S, Robbins D, Schmidt C, Burczak J, Croce CM, Copeland T, Kovatich AJ, Fishel R. hMSH5: a human MutS homologue that forms a novel heterodimer with hMSH4 and is expressed during spermatogenesis. Cancer Res 1999; 59: 816–822.
28. Santucci-Darmanin S, Walpita D, Lespinasse F, Desnuelle C, Ashley T, Paquis-Flucklinger V. MSH4 acts in conjunction with MLH1 during mammalian meiosis. FASEB J 2000; 14:1539–1547.
29. Kolas NK, Svetlanov A, Lenzi ML, Macaluso FP, Lipkin SM, Liskay RM, Greally J, Edelmann W, Cohen PE. Localization of MMR proteins on meiotic chromosomes in mice indicates distinct functions during prophase I. J Cell Biol 2005; 171:447–458.
30. Wei K, Clark AB, Wong E, Kane MF, Mazur DJ, Parris T, Kolas NK, Russell R, Hou H Jr, Kneitz B, Yang G, Kunkel TA, Kolodner RD, Cohen PE, Edelmann W. Inactivation of exonuclease 1 in mice results in DNA mismatch repair defects, increased cancer susceptibility, and male and female sterility. Genes Dev 2003; 17:603–614.
31. Tsubouchi H, Ogawa H. Exo1 roles for repair of DNA double-strand breaks and meiotic crossing over in Saccharomyces cerevisiae. Mol Biol Cell 2000; 11:2221–2233.
32. Khazanehdari KA, Borts RH. EXO1 and MSH4 differentially affect crossing-over and segregation. Chromosoma 2000; 109:94–102.
33. Edelmann W, Cohen PE, Kane M, Lau K, Morrow B, Bennett S, Umar A, Kunkel T, Cattoretti G, Chaganti R, Pollard JW, Kolodner RD, Kucherlapati R. Meiotic pachytene arrest in MLH1-deficient mice. Cell 1996; 85:1125–1134.
34. Lipkin SM, Moens PB, Wang V, Lenzi M, Shanmugarajah D, Gilgeous A, Thomas J, Cheng J, Touchman JW, Green ED, Schwartzberg P, Collins FS, Cohen PE. Meiotic arrest and aneuploidy in MLH3-deficient mice. Nat Genet 2002; 31:385–390.
35. Woods LM, Hodges CA, Baart E, Baker SM, Liskay RM, Hunt PA. Chromosomal influence on meiotic spindle assembly: abnormal meiosis I in female Mlh1 mutant mice. J of Cell Biol 1999; 145:1395–1406.
36. Hodges CA, LeMaire-Adkins R, Hunt PA. Coordinating the segregation of sister chromatids during the first meiotic division: evidence for sexual dimorphism. J Cell Sci 2001; 114:2417–2426.
37. Tarkowski AK. An air-drying method for chromosome preparations from mouse eggs. Cytogenetics 1966; 5:394–400.
38. Yuan L, Liu JG, Zhao J, Brundell E, Daneholt B, Hoog C. The murine SCP3 gene is required for synaptonemal complex assembly, chromosome synapsis, and male fertility. Mol Cell 2000; 5:73–83.
39. Yuan L, Liu JG, Hoja MR, Wilbertz J, Nordqvist K, Hoog C. Female germ cell aneuploidy and embryo death in mice lacking the meiosis-specific protein SCP3. Science 2002; 296:1115–1118.
40. Tran PT, Erdeniz N, Symington LS, Liskay RM. EXO1-A multi-tasking eukaryotic nuclease. DNA Repair (Amst) 2004; 3:1549–1559.
41. Tran PT, Fey JP, Erdeniz N, Gellon L, Boiteux S, Liskay RM. A mutation in EXO1 defines separable roles in DNA mismatch repair and post-replication repair. DNA Repair (Amst) 2007; 6:1572–1583.
42. Amin NS, Nguyen MN, Oh S, Kolodner RD. exo1-dependent mutator mutations: model system for studying functional interactions in mismatch repair. Mol Cell Biol 2001; 21:5142–5155.
43. Guillon H, Baudat F, Grey C, Liskay RM, de Massy B. Crossover and noncrossover pathways in mouse meiosis. Mol Cell 2005; 20:563–573.